STRUCTURAL CHARACTERIZATION OF LITHIUM DOPED NZP $Na_{1-x}Li_xZr(PO_4)_3$(x=0.00-0.75)

[1]Ahmadu U*., [2]Musa A. O., [3]Rabiu N. and [4]Nuntanwong N.
[1]Department of Physics, Federal University of Technology, Minna, Nigeria
[2] Department of Physics, Bayero University, Kano, Nigeria
[3]Department of Physics, Ahmadu Bello University, Zaria, Nigeria
[4]National Electronics and Computer Technology Centre, Thailand
*Correspondence author: u.ahmadu@yahoo.com

ABSTRACT
Sodium zirconium phosphate (NZP) of composition $Na_{1-x}Li_xZr_2(PO_4)_3$ (x=0.0-0.75) have been synthesized using solid state reaction, with a view to minimizing the ZrO_2 second phase normally present .The compositions have been characterized by XRD and SEM for phase composition, lattice parameters and density. No ZrO_2 second phase was detected in some of the compositions, rather $Na_sZr(PO_4)_3$ and the density showed a systematic decrease with increase of Li. All The compositions belong to the rhombohedral crystal system and were indexed based on hexagonal lattice structure. The density of the composition x=0.00 as calculated from the XRD data is $3.02g/cm^3$.The grain sizes of the compositions are in the range 1-2µm, 2-5µm, 3-7µm and 2µm for x=0,0.25,0.5 and 0.75, respectively.
Keywords: solid state synthesis, NZP, XRD

INTRODUCTION
Sodium zirconium phosphate is one of the most studied materials in recent times. The compound has general formula $NaZr_2(PO_4)_3$ and is the main framework structure for a broad spectrum of compositions known as NASICON (sodium superionic conductor), $Na_{1+x}Zr_{2-x}P_{3-x}Si_xO_{12}$, x=0-3.The compounds have special structural features such that all the atoms, except oxygen, can be substituted by various atoms of differing oxidation states and radii, giving the resulting compositions different chemical and physical properties, while at the same time retaining the main crystal structure. They have potential use as rechargeable lithium ion batteries, nuclear waste immobilizers, environmental sensors, thermal shock resistant materials, with thermal expansion tailorability, among many other applications (Brunet *et al*, 2003; Jasinski, *et al*, 2005). The synthesis of the materials using solid state reaction inevitably leads to the precipitation of ZrO_2 second phases (Aono, 1994; Lee *et al*, 2004).The heat treatment times leading to the formation of the compounds involves various time and temperature tradeoffs for calcination and sintering (Kumar and Yashonath, 2006; Naik *et al*, 2004; Agrawal *et al,* 2006; Naik *et al*,2010). Many studies targetted the synthesis of the compositions at low temperatures (Bothe and Brown, 2005) using solid state reaction and sol-gel method, for example. On the other hand reducing the heat treatment periods. This has lead to improved grain formation in microstructure and the enhancement of other physical and chemical properties of the compositions (Naik *et al*, 2004; Fuentes *et al,* 2004). In this work we report a total of 8 hrs for each stage of the processing at a temperature of 1523K(1250°C), using X-ray diffraction

and scanning electron microscopy studies. Pet'kov *et al*, (2003) characterized the structure and thermal properties of the composition $Na_{1-x}Li_xZr_2(PO_4)_3$, x=0.0,0.3 and 0.5. In this work we report in detail the structure, lattice parameters, density and crystallite size of the compositions up to x=0.75.

MATERIALS AND METHODS
The samples were prepared using solid state synythesis. Basic materials of analytical grade (> 99%) that were used are: $Na_2CO_3.H_2O$, ZrO_2, Li_2CO_3 and $NH_4H_2PO_4$. Stoichiometric amounts of these materials were mixed and thoroughly ground in an argate mortar for about five hours.The samples were then dried in air for about four (4) hours. Acetone was added in appropriate quantity to homogenize the mixture. Pellets of discs of 13mm diameter and 6mm thickness were prepared for sintering under pressure of $7.42 \times 10^6 N/m^2$. The powder samples were placed inside a gas-heated furnace for eight hours at successive temperatures 573, 773, 1323,1373,1423K,1473 and 1523K, respectively. A detailed description of the sample preparation and synthesis has been presented elsewhere (Ahmadu *et al*, 2010). Specimens of the sintered powder were characterized by X-ray diffraction measurements using a precision mini XRD difractometer MD-10, Version 2.0.4 by Radicon Ltd. The 2θ range used was 16-70° and the working power was 25kV, using 20 minutes acquisition time and CuKα radiation λ =1.5406Å. The calibration standard used was Corundum. Four compositions of the sintered samples were subjected to XRD measurements, and the analyses of the XRD data was carried out using Microsoft EXCEL Program.

SEM micrographs were obtained using a small power 5kV TMEC scanning electron microscope machine at different magnifications, from 4000 to 20,000 on sintered specimen samples of $Na_{1-x}Li_xZr_2(PO_4)_3$.

RESULTS AND DISCUSSIONS
Phase, Structure and Lattice Paramaters
The XRD patterns for all the compositions are presented in fig. 1-4 for compositions x = 0.00, 0.25, 0.50 and 0.75, respectively. Fig. 5 shows the same patterns plotted on the same scale for comaparison. The XRD patterns are identical to the ICDD-PDF (International Crystal

Diffraction Data-Powder Diffraction File) patterns in all compiositions, and are mainly in single phase, with presence of minor phase of tetragonal ZrO_2. No unreacted starting materials were detected, an indication that the reaction was complete. The results show that the samples are polycrystalline and the composition x= 0.00 (fig.1) has the additional minor phases of ZrO_2 (tetragonal) and a liquid–like (glassy) monoclinic $NaPO_3$,which can be seen in the diffuse peaks at high 2θ values, from 55^0 and above.
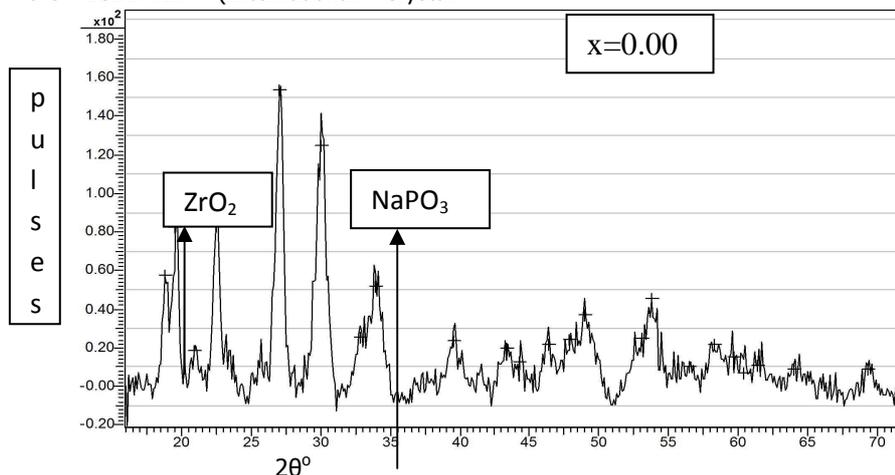
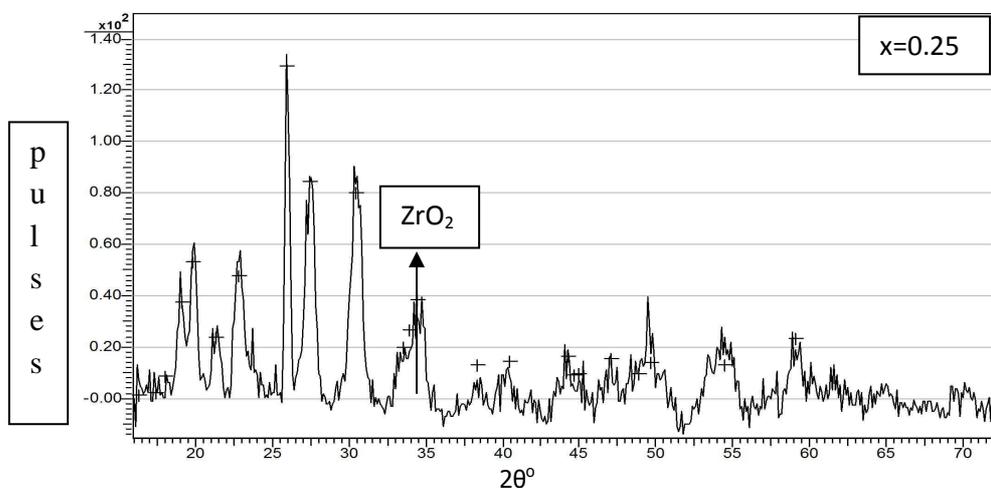**Fig. 1: XRD pattern of sintered sample x =0.00 with ZrO₂ and NaPO₃ additional phases.**

These phases are represented (as calculated and from the XRD data) by the d-lines at 33.99^o and 48.96^o ,respectively (where d in is the interplanar spacing,). ZrO_2 is normally precipitated in solid state reactions (Kang and Cho,1999; Fuentes *et al*, 1999; Lee *et al*, 2004; Nga and Son, 2004) due to the high temperature used, resulting in the segregation of Zr^{4+} during volatilization of Na and P at the grain boundaries (Fuentes *et al,* 2004; Lee *et al,* 2004). The $NaPO_3$ is a glassy material observed in the synthesis of NASICON (Lee *et al*, 2004) and reported to act as flux in the grain boundaries and enhances sinterability (Lee *et al*, 2004; Forsyth *et al*, 1998). The patterns generally have their 2θ values similar with slight shifts as more substitution of Na by Li is effected.

The theoretically calculated and the experimentally observed d-spacings are very close, an

indication that indexing the crystal system on the hexagonal lattice was appropriate. At 2θ=33.99°, 48.96° there was coexistence of ZrO_2 (with relatively intense peak) and $NaPO_3$ phases in addition to the NZP, respectively. These are minor impurity phases since there are no other peaks and therefore their effect is minimal. The intensity of the peaks is seen to increase smoothly with increasing x, wher x=0.75 has the highest intensity. This directly reflects the effect of increasing substitution of Lithium on the unit cell parameters. The micrograph for sample x=0.25 is depicted in fig. 2 and shows well formed grains of large size with a narrow range of size distribution of about 2-5 μm. The bright spots are tetragonal ZrO_2 and $Na_5Zr(PO_4)_3$ detected by XRD.

Fig. 2: XRD pattern of sintered sample x=0.25 with only one phase , ZrO₂.

The pattern for the sample x=0.50 is shown in fig. 3 with the phase $Na_5Zr(PO_4)_3$, at 27.12°, but no presence of ZrO_2 was detected, showing that the synthesis was very complete.
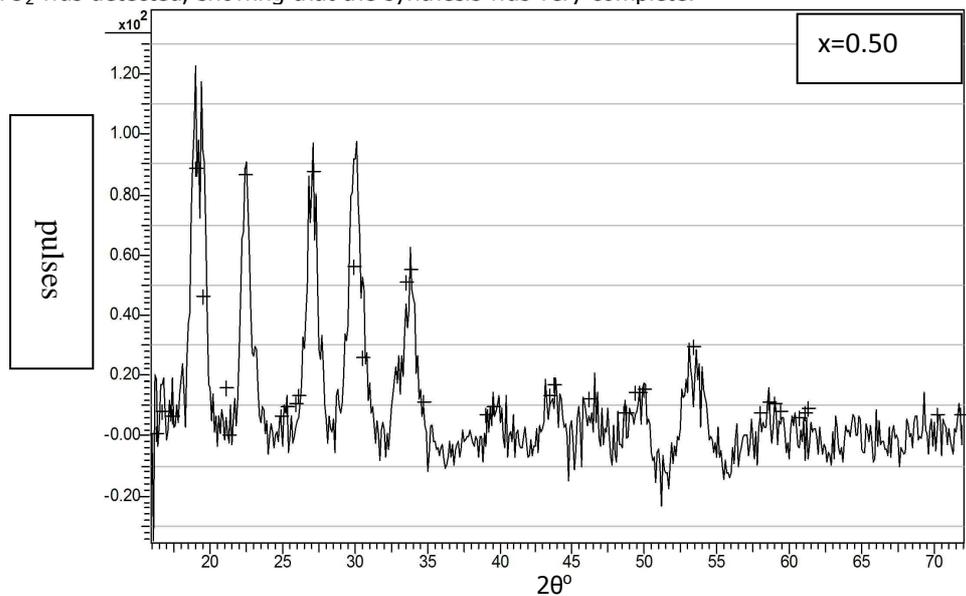

Fig. 3: XRD pattern of sintered sample x= 0.50 with additional phase of,$Na_5Zr(PO_4)_3$.

The last sample, x=0.75, shown in fig.4 4.9(d) also has only the phase $Na_5Zr(PO_4)_3$ coexisting with the NZP material and has the highest intensity for 2θ values.
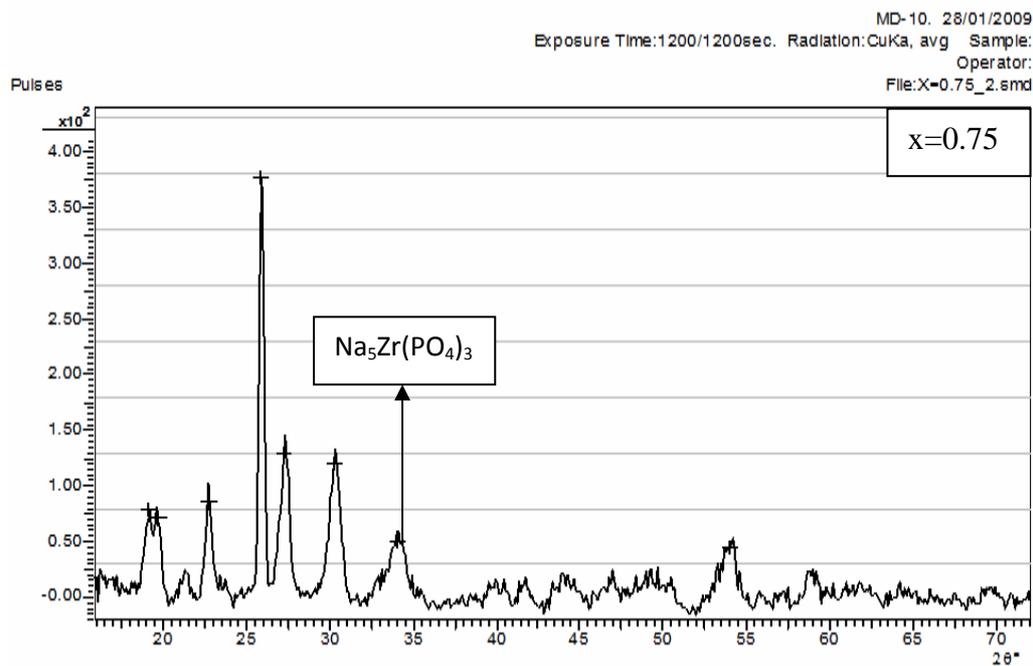

Fig. 4: XRD pattern of sintered sample x= 0.75 with additional phase of $Na_5Zr(PO_4)_3$

All the compositions belong to the rhombohedral crystal system with the R-3c space group based on a hexagonal unit cell lattice. Impurity phases had been detected in some compositions in the study of $Li_{1+x}Ga_xTi_{2-x}(PO_4)_3$(x=0.1-0.9) in which it was demonstrated that these do not affect the electrical properties of the material (Oda *et al*, 2007). Table 1 is a summary of the most important results determined from the XRD data: lattice parameters, densities (theoretical and calculated), average crystallite size, calculated from the Scherer equation , in comparison with published data.

The calculated lattice parameters, based on indexing on a hexagonal lattice from the ICDD data base PDF-2(33-1312), has 80 reflections It shows that the composition x=0.00 belongs to the rhombohedral crystal system with a hexagonal unit cell lattice, where a =8.8048Å = b and c = 22.7572Å, $α=β=90^o$ and $γ =120^o$ and a density of 3.198g/cm³.The result from the present work, Kotelnikov e*t al* (2001), Pet'kov *et al* (2003) and Kotelnikov *et al* (2009) are shown in table 1 for comparison.

Fig. 5 is the composite plot of the XRD data on the same scale. The 2θ values of the peaks, for all compositions fall virtually on the same point, except for slight shifts due to the substitution of Na by lithium and the consequent changes in unit cell dimensions, as expected (Forsyth *et al*, 1998). The summary in table 1 shows that the result from the present work is highest in the lattice parameter a than all the references for compossition x=0.00. It is also larger than that of other comparative compositions, 0.50 and 0.70, from Pet'kov *et al* (2003). This may be due to a systematic error resulting from the inability to perform the XRD in step scan mode, thereby causing some of the reflection peaks to be missing (particularly from the lower 2θ values) since these are important in the determination of the lattice parameter a. It has been observed that a shift in 2θ values, towards lower values, could be as a result of ion difference between dopants with higher ion radius than host (Wu, 2005). However, since this is pristine composition such a situation is not expected, though Mouahid *et al* (2001) have reported a case in which Al , which was intended for substitution at the octahedral sites of NASICON, was also detected at the tetrahedral sites, with implications for stoichiometry and unit cell dimensions. Further investigations are required to confirm this. It is noteworthy that the crystallite size for x=0.00 was the smallest, 1.87Å and could have affected the accuracy of the 2θ values obtained in fig5.

The variation of the relative values of the lattice parameters a and c for sample x=0.00 are shown in Fig. 6-7 with their error bars. It can be seen that while the a parameter was systematically higher, the c parameter, on the other hand, was smaller. It is possible that it is due to the synthesis characteristics, such as microcracking, although the grain size for the sample is less than the critical size for the phenomenon to be observed. Increasing incorporation of Li^+ cation into the appropriate lattice is supposed to decrease the c parameter. However, further incorporation is expected to increase the a parameter, due to the contraction of the structure in the c direction, with its subsequent extension in the a direction. A similar but reverse of this investigation (substitution of Potassium, K, of larger radius than Na, Li) has been studied by Pet'kov *et al (*2003), where potassium was substituted for Na in $NaZr_2(PO_4)_3$, though specific analysis of the Na occupancy sites was not available, as a full structural analysis was not carried out.

Their results showed that the effect of substitution and the subsequent variation was not smooth in terms of increasing c parameter with increase in K content (Kotelnikov *et al*, 2001 ; Pet'kov *et al*, 2003). At a particular composition, a decrease in a was observed on the contrary, due to the position Potasium, K may occupy on the possible occupancy sites. Fig. 8 shows that with increase in lithium, the cell volume initially decreased (x=0.25), then at a particular composition x, it increased and subsequently decreased as x increased to the maximum. The increase in cell volume may be explained in terms of the site occupancy of the Li and Na ions. If both are on the same site, say on the MI site, there should be an increment in the c axis, with a corresponding decrease in a axis. This could lead to the 'mixed cation effect' with subsequent implication for the electrical conductivity of the sample.

Fig. 9 is a plot of the variation of lattice parameters a and c with increase in lithium content for all the compositions. It shows that there is little variation in lattice parameters with increase in lithium content. At about x=0.25 we observe a slight decrease in both a and c parameters. There are rare reports of coupled mobile ion in NASICON systems, in particular the effect of their substitution on site occupancies. One such report on Na-Li exchange of $Na_{1+x}Ti_{2-x}Al_x(PO_4)_3$(0.6≤$x$≤0.9) NASICON series, showed that partial Li exchanges (substitutions) in the system leads to a decrease in the length of the a axis, whereas the change in the c-axis is negligible as it is more sensitive to the MI site. Further, the Li was found located in the MII site while the MI site has both Na and Li. However, in the fully exchanged samples, the c axis decreased while the a axis increased (Mouahid *et al*, 2001). It should be noted that in the NASICON system, the MI site is completely filled by Na ions while the MII site is empty. This is also the case here, although there is less degree of change in the lattice dimensions since the substitution are limited to x=0.75.

The theoretical density of composition at x=0.00 is 3.20g/cm³ and was very close to that calculated from the XRD data which is 3.02g/cm³.The result obtained from experimental data by measuring the dimensions of the pellet was however lowest for the x=0.00 sample, i.e. 1.94g/cm³, with a degree of compaction of about 61%. This may be attributted to the sintering conditions and microstructure of the compounds, though porosity was not observed to explain the low density. Fig.10 depicts the variation of the average density of the samples (calculated from the XRD data) against the compositions, which should be understood within the context of the variation of the unit cell volume earlier discussed. The initial increment in the density is in accordance with the decrease in the unit cell volume observed for x=0.25. Subsequently however, there is a decrease in density with further lithium incorporation which is attributted to the lower density of lithium compared to Na.

Table 1: Summary of X-ray diffraction results for Na$_{1-x}$Li$_x$Zr$_2$(PO$_4$)$_3$(x =0.00-0.75) showing the lattice parameters and reference compositions, together with that of LiZr$_2$(PO$_4$)$_3$(x=1.00).

| Sample	Lattice Parameters		V	d$_{x-ray}$	d-cal	Average	Reference
	a, Å	c, Å	Å^3	g/cm^3	g/cm^3	Crystallite size Å	
x =0.00	9.0796±0.0471	22.6960±0.0765	1618.8431	3.02±0.05	1.94(61%)	1.8666	Present Work
	8.803(1)	22.764(1)	1527.8(2)	-	-	-	Kotelnikov *et al* (2001)]
	8.8000	22.8600	1534	-	-	-	Pet'kov *et a l* (2003), Kotelnikov *et al*, 2009
	8.8048	22.7572	1527.88	3.20	-	-	ICDD, PDF-2(33-1312)
x =0.25	8.9661±0.0257	22.4466±0.0824	1563.0683	3.10±0.05	2.16(68%)	15.0687	Present Work
x=0.30	8.7780	23.2580	1552	-	-	-	Pet'kov *e t al* (2003)
x=0.50	9.1153±0.0558	22.7457±0.1336	1626.61982	2.92±0.03	2.12(67%)	2.3016	Present Work
x=0.50	8.7630	23.4590	1560	-	-	-	Pet 'kov *et al* (2003)
x =0.75	9.0291±0.0260	22.5647±0.0782	1588.48314	2.98±0.03	-	2.3090	Present Work
x=0.70	8.7420	23.6980	1568	-	-	-	Pet'kov *et al* (2003)
LiZr$_2$(PO$_4$)$_3$	8.8077	22.7150	1526.05	3.10	-	-	Salkus *et al* (2006)
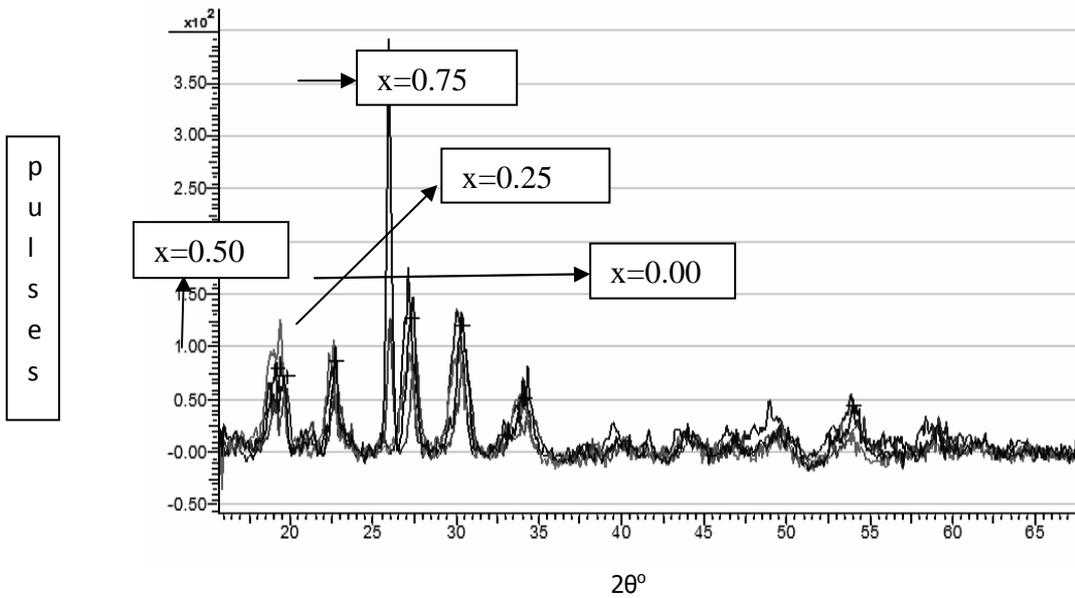
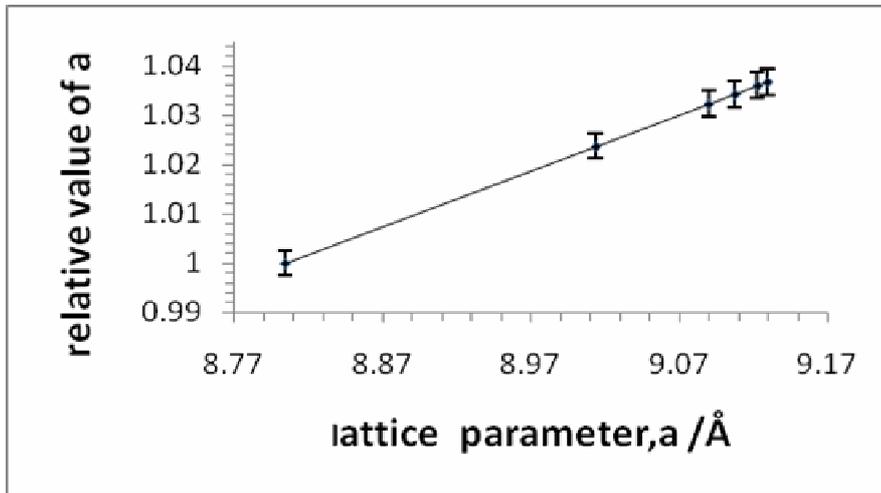Fig. 5: Composite XRD patterns of sintered samples of $Na_{1-x}Li_xZr_2(PO_4)_3$ on the same scale for x=0.00-0.75.

Fig. 6: Relative values (with respect to PDF-2:33-1312) of lattice parameter a plotted against the XRD determined lattice parameter and their error bars for sample x=0.00.
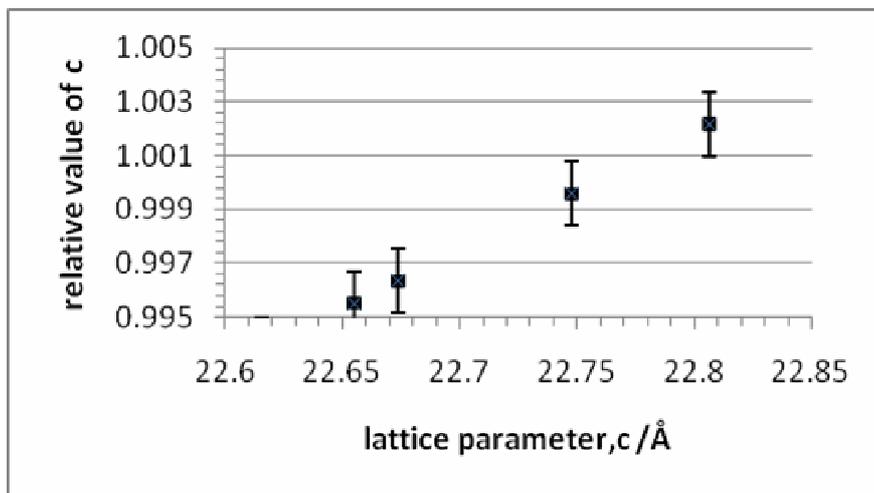

Fig. 7: Relative values (with respect to PDF-2:33-1312) of lattice parameter c plotted against the XRD determined lattice parameter and their error bars for sample x=0.00.
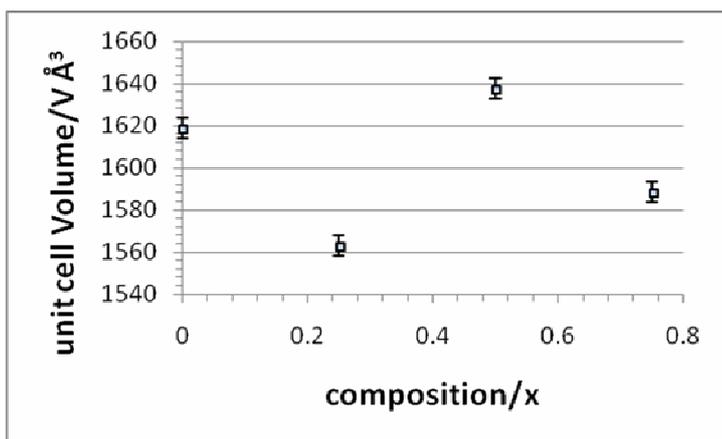
Fig. 8: Variation of unit cell volume versus composition and the error bars for sample x=0.00-0.75.
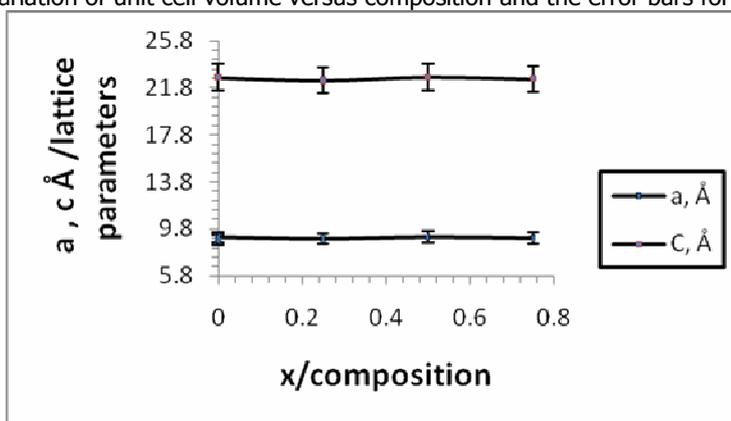

Fig. 9: Plots of experimentally determined lattice parameters a and c against composition(x) with error bars for samples x=0.00-0.75.
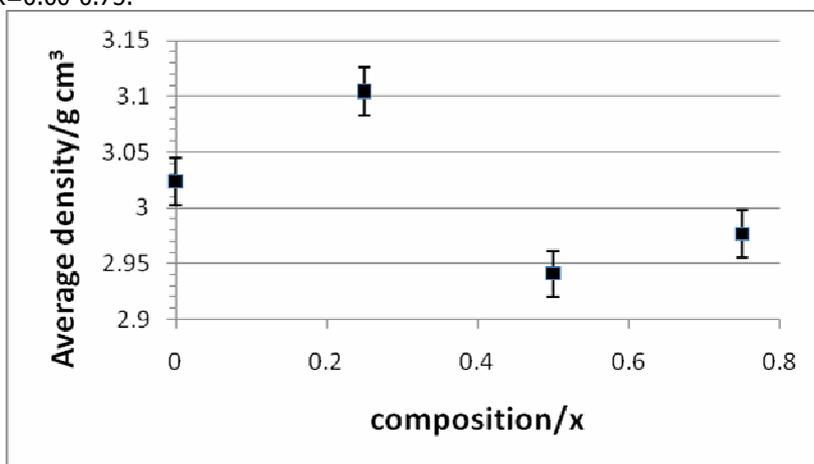

Fig. 10: Variation of density with composition and error bars for sample x=0.00-0.75.

The result of the effect of the substitutions of Na by K (larger radius) of selected compositions, on lattice parameters and density, has also been provided for comparison in table 1 from Pet'kov *et al* (2003). The densities showed a decrease with increasing incorporation of lithium which should be expected due to the lower density of lithium compared to Na that is being replaced. The value of lattice parameter c however, generally decreased with increasing lithium incorporation, which should be expected too as Li has smaller ionic radius than Na. The value should be contrasted with that from the total substitution of Li in

the system given by the lattice parameters from Salkus *et al* (2006) of $LiZr_2(PO_4)_3$,(i.e. x=1.0), which is further evidence that the x=0.75 composition's c parameter is appropriate. The volume V of the unit cell should actually decrease with increasing substitution of Li in the system, however it is generally higher because of the consistently high values of the a parameter which made the volume of the cell to increase instead. The average crystallite size calculated from the Scherer's formula for the x=0.00 composition is 1.8666Å.

Wheaeas the composition x=0.25, with crystallite size of 15.0686Å is the largest and expectedly gave a more accurate result, in terms of the lattice parameters, where a=8.966Å and c =22.446Å. Similarly, it is expected to have the highest electrical conductivity due to the largeness of its crystallite size.

Microstructure Determination
The microstructure results for sample x=0.00 is shown in fig.11, showing liquid-like phases, which were confirmed by XRD to be glassy $NaPO_3$ and at the top and right hand corners are also seen well grains small grains between 1-2µm. The bright crystallites are tetragonal ZrO_2. Many studies have observed the presence of monoclinic ZrO_2 instead, which could be attributted to the sintering temperature used. It has also been reported that phase formation at lower temperatures often leads to smaller grain sizes (Simmer *et al*, 1998) and that the particle with lower particle size has the lower crystallite size.
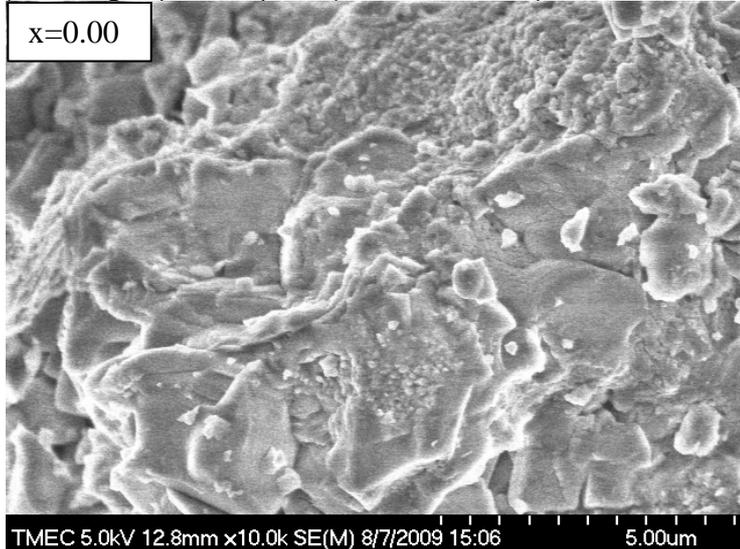

x=0.00

TMEC 5.0kV 12.8mm ×10.0k SE(M) 8/7/2009 15:06   5.00um

Fig. 11: Micrograph of sintered sample x=0.00 with liquid–like phases and well formed crystallites at the top left corner.

The micrograph for sample x=0.25 is depicted in fig. 12. It shows grains of large size with a narrow range of size distribution, 2-5 µm with very few pores. The bright spots are tetragonal ZrO_2 and $Na_5Zr(PO_4)_3$ detected by XRD. The crystallite size is largest, consistent with the particles sizes in the SEM.

x=0.25

TMEC 5.0kV 12.8mm ×11.0k SE(M) 8/7/2009 15:16   5.00um
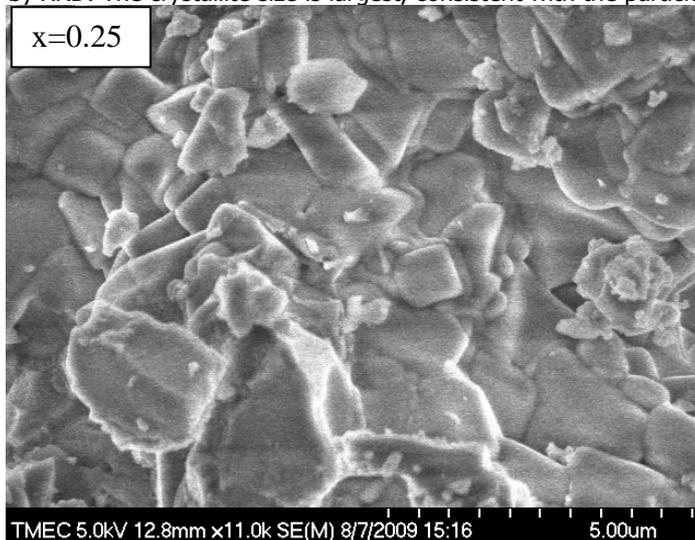
Fig. 12: Micrograph of sintered sample x=0.25 showing well formed grains of different sizes and virtually no porosity .

The SEM micrograph for sample x=0.50 is depicted in fig.13. It has larger grain size, little pores and well grains. One can also observe a fairly narrow size distribution, in the 3-7µm range, with no trace of ZrO_2, rather the presence of $Na_5Zr(PO_4)_3$, as detected in the XRD results.
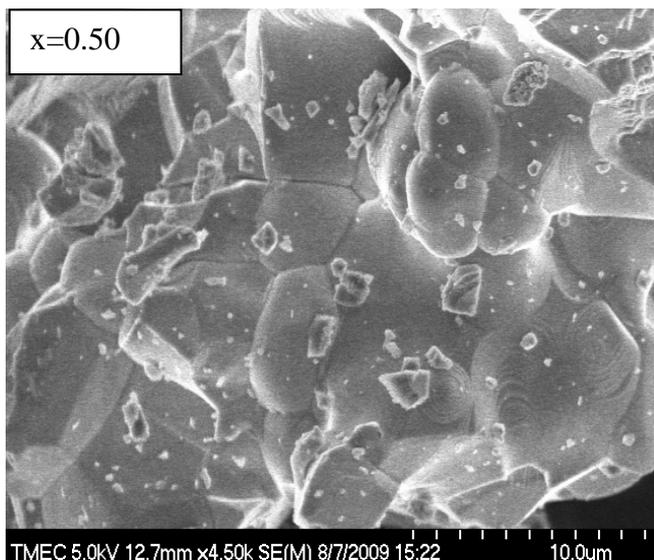
142

Fig. 13: Micrograph of sintered sample x=0.50 showing large grains and and without porosity.

The last sample, x=0.75 in fig. 14 also shows a fairly large grain size of about 2μm with a wider size distribution in accordance with its crystallite size of approximately 2.3Å. There was also no ZrO_2, though a peak belonging to $Na_5Zr(PO_4)_3$ was detected. It appears that lithium substitution favours grain growth with increasing Ga^{3+} substitution, a characteristic observed in the study of $Li_{1+x}Ga_xTi_{2-x}(PO_4)_3$(x=0.1-0.9) by Oda *et al* (2007).
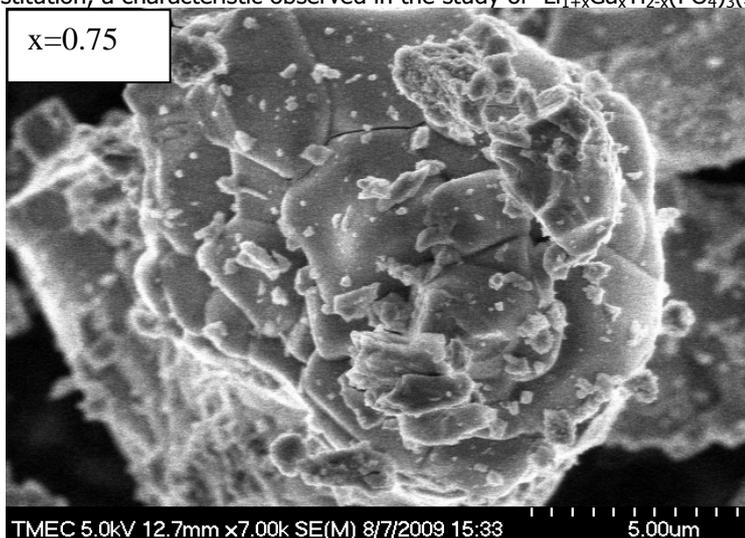

Fig. 14: Micrograph of sintered sample, x=0.75 with grains of about 2 μm size.

CONCLUSION

The four compositions of $Na_{1-x}Li_xZr_2(PO_4)_3$,x=0-0.75 were characterized by X-ray diffraction for phase, structure, density and crystallite size. The compositions were mainly single phase with minor phases of ZrO_2 and $Na_5Zr(PO_4)_3$. The crystal system of all the compositions showed that they belong to the rhombohedral crystal system of the R-3c space group and were indexed based on hexagonal lattice structure. Although it was observed that the lattice parameter 'a' was higher than that reported in literature for composition x=0.00, the c parameter was within the range obtained for the compositions and showed a fairly linear relationship with increasing incorporation of lithium. The high value was attributed to several factors, among which is the inability to perform the XRD scan at a lower rate (step scan mode). However, the theoretical densities calculated from the lattice parameters were close to the standard values. The computed experimental densities were close to 70% in some compositions showing that the degree of densification attained was relatively high. Comparable data or literature was not available for compositions other than x=00 and x=0.50.

REFERENCES

Agrawal, D., Cheng, J., Fang ,Y. and Roy, R. (2006). Microwave processing of ceramics, composites and metallic materials. *In*: Clark, D. E., Folz, D. C., Fogar, C. E. and Mahmoud, M. M. (Eds), *Microwave solutions for ceramic engineers*. The American ceramic society, Ohio,USA. p.213.

Ahmadu, U., Musa, A.O., Jonah, S.A. and Rabiu, N. (2010). Synthesis and thermal characterization of NZP compounds $Na_{1-x}Li_xZr_2(PO_4)_3$ (x=0.00–0.75). *Journal of Thermal Analysis and Calorimetry,* 101:175-179.DOI 10.1007/s10973-010-0679-y.

Aono, H. (1994). Studies On Li^+ ionic conducting solid electrolyte composed of Nasicon-type structure. PhD. Thesis. Osaka University, Japan.p.8.

Bothe, J.V. and Brown. (2005). Low temperature formation of NZP ceramics: http://www.netl.doe.gov/publications/proceedings/03/ucr-hcbu/Brown/pdf. Retrieved December, 2009.

Brunet, F., Bagdassarov, N. and Miletich, R. (2003). $Na_3Al_2(PO_4)_3$, a fast sodium conductor at high pressure: in-situ impedance spectroscopy characterization and phase diagram up to 8 GPa. *Solid State Ionics,* 159:35-47.

Forsyth, M., Wong, S. Nairn, K.M., Best, A.S., Newman, P.J. and MacFarlane,

D.R. (1998). NMR studies of modified Nasicon-like, lithium conducting solid electrolytes: http://www.eng.hawaii.edu/¬ssi II/SSI-II papers/C55/C55.pdf. Retrieved, August, 2009.

Fuentes, R.O, Marques, F .M. B. and Franco, J .I. (1999). Synthesis and properties of nasicon prepared from different zirconia-based precursors. *Boletin de la sociedad Espanola de Ceramica Y Vidrio. V,* 38:631-634.

Fuentes, R.O., Lamas, D.G., Fernandez de Rapp M.D., Figueiredo, M. N., Frade, J.R., Marques, F. M. B. and Franco, J. I. (2004).Restrictions to obtain NASICON by a ceramic route. *Boletin de la sociedad Espanola de Ceramica Y Vidrio V,* 43: 775-779.

Jasinski, G., Jasinski, P., Chachulski, B., Nowakowski, A. (2005). Lisicon Solid Electrolyte Electrocatalytic gas sensor. *Journal of the European Ceramic Society*, 25:2969.

Kang, H. and Cho, N. (1999). Phase Formation ,Sintering behavior, and electrical characteristics of NASICON compounds. *Journal of Materials Science*, 34:5005-5013.

Kotelnikov, A.R., Kovalskii, A.M., Karyaeva E.G., Orlova, A.I. ,Pet'kov, V.I., Akhmedzanova, G.M. and Ushakovskaya, T.V.(2001). Investigation of (Na,Sr)-Zirconium

Phosphate solid solutions: http://www.libray.iem.ac.ru.exper/V8_2/six .pdf. Retrieved,December, 2008.

Kotelnikov, A.R., Kovalskii, A.M., Karyaeva, E.G., Orlova, A.I., Petkov, V.I., Chichagove, A.V., Ushakovskaya, T.V. and Ulin I.V. (2009). Investigation of (Na, K)-zirconium-phosphate experimental study. *Crystal growth, structure and physical properties of crystals,* 7: 68-69.

Kumar, P.P. and Yashonath, S. (2006). Ionic conduction in the solid state. *Journal of Chemical Science,* 118(1):135-154.

Mouahid F.E., Zahir M., Maldonado-Manso P.M., Bruque S., Losilla E.R., Aranda M.A.G., Rivera A, Leona C, Santamaria J. (2001). Na-Li exchange of $Na_{1+x}Ti_{2-x}Al_x(PO_4)_3 (0.6 \leq x \leq 0.9)$ NASICON series: a Rietveld and impedance study. *Journal of Material Chemistry,*11:3258-3263.

Petkov, V.I., Orlova, A.I., Trucbach, I.G., Asabina, Y.A., Demarin, V.T. and Kurazhkovskaya, V.S. (2003a). Immobilization of nuclear waste materials containing different alkali elements in single-phase NZP-based ceramics. *Czechoslovak Journal of Physics,* 53: A639-A648.

Lee, J.S., Chang, C.M., Lee, Y.I., Lee, J.H. and Hong, S.H. (2004). Spark plasma sintering (SPS) of NASICON Ceramics. *Journal of American Ceramic Society*, 87:305-307.

Naik, A.H., Thakkar, N.V., Darwatkar, S.R., Mudher, K.D.S., Venagopal, V.V. (2004). Microwave assisted low temperature synthesis of sodium zirconium phosphate ($NaZr_2(PO_4)_3$). *Journal of Thermal Analysis and Calalorimetry,* 76:707-713.

Naik, A. H., Deb, S. S, Chalke, A. B., Saxena, M. K., Ramakumar, K. L.,

Venugopal, V. and Dharwadkar, S.R. (2010). Microwave-assisted low temperature synthesis of sodium zirconium Phosphate (NZP) and the leachability of some selected fission products Incorporated in its structure–a case study of leachability of caesium. *Journal of Chemical Science,* 122: 71–82.

Nga, N.T. and Son T. (2004). Interaction model of the interface NASICON with aqueous solution. *Communication in Physics*, 4:105-110.

Oda, K. Takase, S. and Shimizu, Y. (2007). Preparation of high conductive lithium ceramic. *Material Science Forum*, 544-5:1033-1036.

Salkus, T., Dindune, A. ,Kanepe, Z. Ronis, J. Kazeonis, A. and Orliukas, A. E. (2006). Synthesis Structure and Electric properties of $L_{1+x}Sc_xZ_{2-x}(PO_4)_3$(x=0.1,0.2,0.3). *Lithuanian Journal of Physics, 46*:361-366.